The development of the cloaca in the human embryo

Nutmethee Kruepunga,[1,2] Jill P. J. M. Hikspoors,[1] Hayelom K. Mekonen,[1] Greet M. C. Mommen,[1] Krai Meemon,[2] Wattana Weerachatyanukul,[2] Somluk Asuvapongpatana,[2] S. Eleonore Köhler[1] and Wouter H. Lamers[1,3] (iD)

[1]*Department of Anatomy & Embryology, Maastricht University, Maastricht, The Netherlands*
[2]*Department of Anatomy, Faculty of Science, Mahidol University, Bangkok, Thailand*
[3]*Tytgat Institute for Liver and Intestinal Research, Academic Medical Center, Amsterdam, The Netherlands*

Abstract

Subdivision of cloaca into urogenital and anorectal passages has remained controversial because of disagreements about the identity and role of the septum developing between both passages. This study aimed to clarify the development of the cloaca using a quantitative 3D morphological approach in human embryos of 4–10 post-fertilisation weeks. Embryos were visualised with Amira 3D-reconstruction and Cinema 4D-remodelling software. Distances between landmarks were computed with Amira3D software. Our main finding was a pronounced difference in growth between rapidly expanding central and ventral parts, and slowly or non-growing cranial and dorsal parts. The entrance of the Wolffian duct into the cloaca proved a stable landmark that remained linked to the position of vertebra S3. Suppressed growth in the cranial cloaca resulted in an apparent craniodorsal migration of the entrance of the Wolffian duct, while suppressed growth in the dorsal cloaca changed the entrance of the hindgut from cranial to dorsal on the cloaca. Transformation of this 'end-to-end' into an 'end-to-side' junction produced temporary 'lateral (Rathke's) folds'. The persistent difference in dorsoventral growth straightened the embryonic caudal body axis and concomitantly extended the frontally oriented 'urorectal (Tourneux's) septum' caudally between the ventral urogenital and dorsal anorectal parts of the cloaca. The dorsoventral growth difference also divided the cloacal membrane into a well-developed ventral urethral plate and a thin dorsal cloacal membrane proper, which ruptured at 6.5 weeks. The expansion of the pericloacal mesenchyme followed the dorsoventral growth difference and produced the genital tubercle. Dysregulation of dorsal cloacal development is probably an important cause of anorectal malformations: too little regressive development may result in anorectal agenesis, and too much regression in stenosis or atresia of the remaining part of the dorsal cloaca.

Key words: 3D morphometry; anorectum; bladder; urogenital sinus; urorectal septum.

Introduction

The cloaca is the common compartment of the urogenital and anorectal channels in the 5th developmental week of humans that subdivides into two separate passages during the 6th and 7th weeks. The process of cloacal subdivision has remained controversial even though it has been studied for well over a century. Two main hypotheses exist to account for subdivision of the cloaca. The classical model, which is present in standard textbooks, is the 'active' concept (Carlson, 2014; Moore et al. 2016): a frontally oriented

urorectal septum ('Tourneux's' septum) actively expands caudally to divide the cloaca into its two compartments (Tourneux, 1888; Pohlman, 1911; Quan et al. 2000). The problem with Tourneux's septum has always been that it is shown only as a midline structure without adequate description of its more lateral extension. Alternatively, lateral folds in the wall of the cloaca ('Rathke's' folds) merge in the caudal direction (Rathke, 1832; Retterer, 1890; Reichel, 1893). Although Rathke is credited with the description of the lateral folds, these structures, which are all but invisible in his miniature drawings, are often cited without proper definition of their composition or position. More than 30 years ago, the 'passive' concept was formulated (van der Putte & Neeteson, 1983; Kluth et al. 1995): the urorectal septum extends caudally due to differential growth in the (peri-)cloacal region, which results in 'unfolding' of the caudal body axis of the embryo (van der Putte & Neeteson, 1983; Zhang et al. 2011; Xu et al. 2012; Huang

Correspondence

Wouter H. Lamers, Department of Anatomy & Embryology, Maastricht University, Universiteitssingel 50, 6229 ER Maastricht, The Netherlands. T: +31433881061; E: wh.lamers@maastrichtuniversity.nl

Accepted for publication *13 August 2018*
Article published online *7 October 2018*

et al. 2016). However, apart from the unfolding of the caudal body axis (Paidas et al. 1999), the description of the passive concept has been qualitative thus far. In particular, regional differences in cloacal growth have been implicated, but not yet quantified.

The cloacal membrane and pericloacal mesenchyme (PCM) are important components of the cloacal region. We define the cloacal membrane as that part of the cloacal wall where ectoderm and endoderm have no basal membrane, that is, are indistinguishable. The cloacal membrane is usually described as a thin membrane that eventually ruptures to provide a passage for the urogenital and anorectal channels (Felix, 1912; Kluth et al. 1995; Paidas et al. 1999; van der Werff et al. 2000). However, other studies have described the cloacal membrane as consisting of a well-developed solid mass ventrally ('urethral plate') and a thin cloacal membrane 'proper' dorsally. The urethral plate (also known as 'cloacal plate'; Penington & Hutson, 2002a) expands ventrally and cranially concomitant with the growth of the genital tubercle, whereas the cloacal membrane proper does not grow and eventually even ruptures (Tourneux, 1888; Penington & Hutson, 2002a; Li et al. 2015). These data suggest that the ventral and dorsal parts of the original cloacal membrane have quite different characteristics. In addition, the mesenchymal components in the cloacal region have attracted interest because of their role in regional growth differences that underlie the subdivision of the cloaca according to the passive concept (van der Putte & Neeteson, 1983; Sasaki et al. 2004; Huang et al. 2016).

Visualisation of the cloacal region has proved challenging (Ikebukuro & Ohkawa, 1994; Kluth et al. 2011). The cloaca is usually shown as a midsagittal drawing, with histological sections to support developmental processes in other planes. In addition, the growth pattern in the cloacal region has been globally described (van der Putte, 2004), with most quantitative histological data addressing cell proliferation and apoptosis (Sasaki et al. 2004; Nebot-Cegarra et al. 2005; Matsumaru et al. 2015; Huang et al. 2016). To clarify the growth pattern and the fate of the components of the cloacal region, we reinvestigated the changes in shape of the cloaca, including its lumen, wall and surrounding mesenchyme in human embryos and fetuses between 4 and 10 weeks of development. Changes in size and shape were assessed qualitatively and quantitatively in 3D reconstructions to establish the growth pattern. We report that the cloaca consisted of a ventral 'growing' zone initially sandwiched between cranial and dorsal 'non-growing' zones that account for the changes in cloacal shape during the period studied.

Materials and methods

This study was undertaken in accordance with the Dutch regulations for the proper use of human tissue for medical research purposes. Anonymised specimens from the historical collections of human embryos of the Departments of Anatomy and Embryology, Leiden University Medical Centre (LUMC), Leiden, Academic Medical Centre (AMC), Amsterdam, and Radboud University, Nijmegen, The Netherlands, that were donated for scientific research were included. In addition, digital images of human embryos of the Carnegie collection (Washington, DC, USA) were downloaded from the Digitally Reproduced Embryonic Morphology (DREM) project (http://virtualhumanembryo.lsuhsc.edu).

Image acquisition, 3D reconstruction and visualisation

Well-preserved human embryos and fetuses between 4 and 10 weeks of development were studied (Table 1). The criteria of O'Rahilly as modified in 2010 were used to determine the Carnegie Stage of development and post-fertilisation age of the embryos (O'Rahilly & Müller, 2010; Table 2). We subdivided CS14 into CS14-early, -intermediate and -late because of rapid

Table 1 Sources of human embryos and fetuses.

Stage	Embryo number	Section plane	Source
CS10	S6330	Transverse	DREM
CS11	S6344	Transverse	DREM
CS12	S8943	Transverse	DREM
CS13	S836	Transverse	DREM
CS14-early*	S2201	Transverse	AMC
CS14-intermediate*	S5029	Sagittal	AMC
CS14-late*	S6502	Transverse	DREM
CS15	S2213	Transverse	AMC
CS15	S721	Transverse	DREM
CS16	S5032	Sagittal	AMC
CS16	S6517	Transverse	DREM
CS16	S39	Transverse	LUMC
CS17	S6520	Transverse	DREM
CS18-early	S97	Transverse	LUMC
CS18-late	S4430	Transverse	DREM
CS19	S9325	Transverse	DREM
CS20	S2025	Transverse	AMC
CS20	S462	Transverse	DREM
CS20	S34	Sagittal	LUMC
CS21	S4090	Transverse	DREM
CS22	S983	Transverse	DREM
CS23	S4141	Transverse	AMC
CS23	S9226	Transverse	DREM
CS23	S48	Transverse	LUMC
CS23	S88	Sagittal	RadboudMC
9 weeks	S89	Transverse	LUMC
9.5 weeks	S57	Transverse	LUMC
10 weeks	S1507	Transverse	AMC

*We subdivided CS14 because of rapid developmental changes during this stage.
AMC, Academic Medical Centre, Amsterdam, The Netherlands; CS, Carnegie stage; DREM, Carnegie collection from the Digitally Reproduced Embryonic Morphology project; LUMC, Leiden University Medical Centre, Leiden, The Netherlands; RadboudMC: Radboud Medical Centre, Nijmegen, The Netherlands.
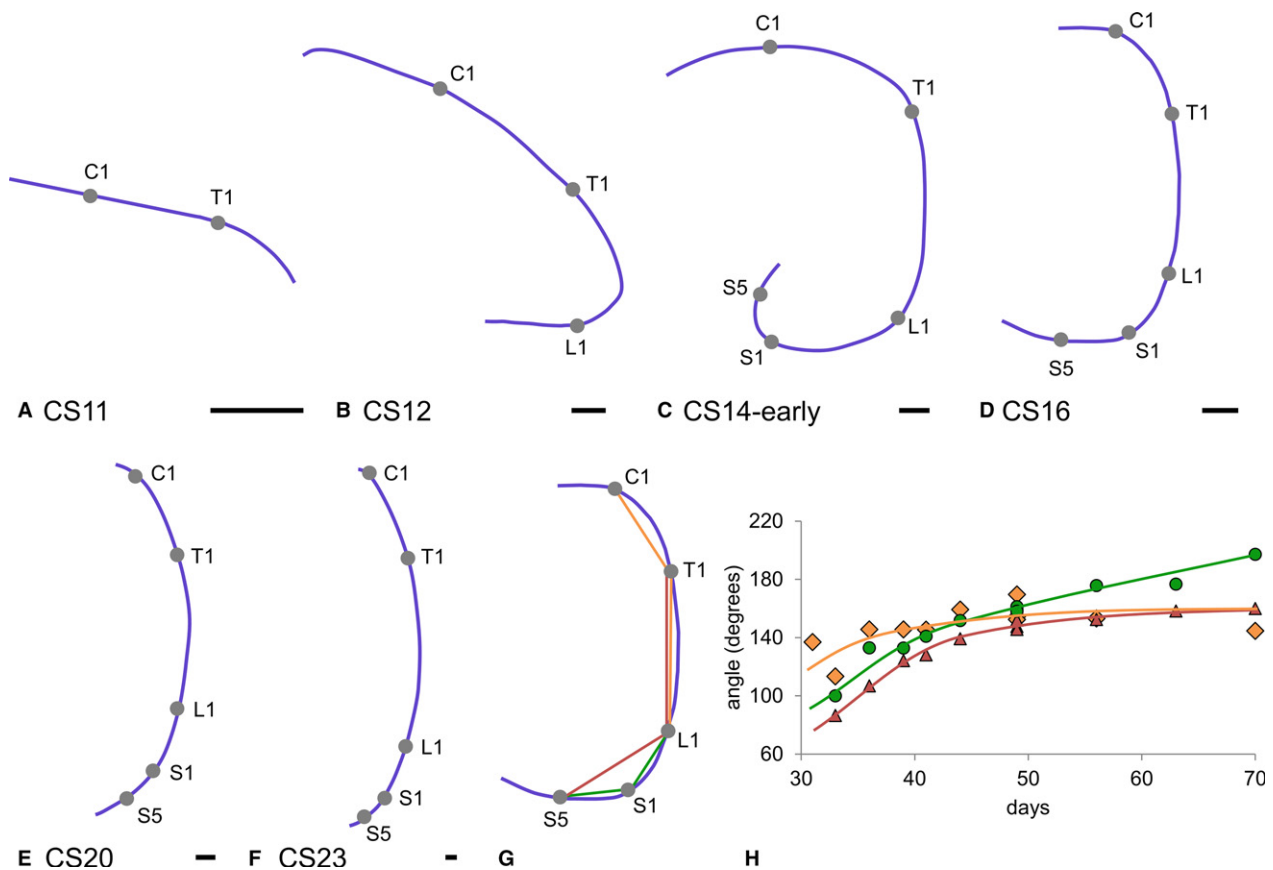
Fig. 1 Curvature of the embryonic axis between 4 and 10 weeks post-fertilisation. Panels (A–F) show left-sided views of the notochord as landmark for the embryonic axis. Panels (A–C) show that, concomitant with the addition of vertebrae (grey dots) up to CS14-early (33 days), the caudal body axis folded ventrally to straighten again between 34 and 42 days (D–F). The angles of C1-T1-L1 (orange diamonds; R^2: 0.62), T1-L1-S5 (red triangles; R^2: 0.97) and L1-S1-S5 (green circles; R^2: 0.94) that quantify this process are shown in (G) and (H). The continuing increase in the L1-S1-S5 angle reflects the development of the sacral promontory. C1, 1st cervical level; T1, 1st thoracic level; L1, 1st lumbar level; S1, 1st sacral level; S5, 5th sacral level. Scale bar: 500 μm.

developmental changes during this stage. The collection from which we selected the embryos studied (Table 2) amounts to ~150 embryos (collections in LUMC and AMC). Selection criteria were histological quality of the sections [embryos undergo autolysis (maceration) quite quickly] and developmental stage. The main limitation to use more embryos was the time required for their 3D reconstruction: scanning and aligning sections remain very time-consuming activities. Instead, we used quantitative (Figs 1 and 5) and qualitative (Figs 2, 6 and 7) chronological development as our most important indicators for adequate description. Accordingly, developmental trends in our account are not based on a single developmental stage. Furthermore, the correlation coefficients that we report are characteristically > 0.8. If a discontinuity or a discrepancy with literature is found, we do check sections of the non-reconstructed group of embryos to confirm our findings.

The serial sections from AMC, LUMC and Radboud were digitised with an Olympus BX51 or BX61 microscope and the Dotslide program (Olympus, Leiderdorp, The Netherlands). All images were converted into grey-scale 'JPEG' format and loaded into Amira3D (version 6.0; base package; FEI Visualization Sciences Group Europe, Merignac Cedex, France). The grey-scale images were aligned automatically with the least-squares alignment mode, and then manually adjusted for correct curvature of the embryonic body axis with the help of photographs and magnetic resonance images of human

embryos of the same stage (Pooh et al. 2011). Structures of interest were segmented manually and reconstructed three-dimensionally with the Amira3D program. Small deformations of individual sections due to the histological processing and stepwise stacking of sections conferred a distracting noise on the 3D reconstructions. Therefore, polygon meshes from all reconstructed materials were exported via 'vrml export' from Amira3D to Cinema 4D (MAXON Computer GmbH, Friedrichsdorf, Germany) and remodelled using the Amira3D model as template. The accuracy of the remodelling process was safeguarded by simultaneous visualisation in Cinema 4D of the original output from Amira and the remodelled Cinema model (Fig. S1). The Cinema-4D models were transferred via 'wrl export' to Adobe Acrobat version 9 (http://www.adobe.com) to generate interactive 3D Portable Device Format (PDF) files, which are an easily accessible format for 3D visualisation (Figs S1 and S4–S6).

Measurements

All morphometric analyses were performed in Amira3D. Analyses included angles between landmarks on the vertebral column, topographic position of landmarks, and distances between landmarks. The data were subsequently analysed in Microsoft Excel (Microsoft, Washington, USA). We used nine landmarks: (i)
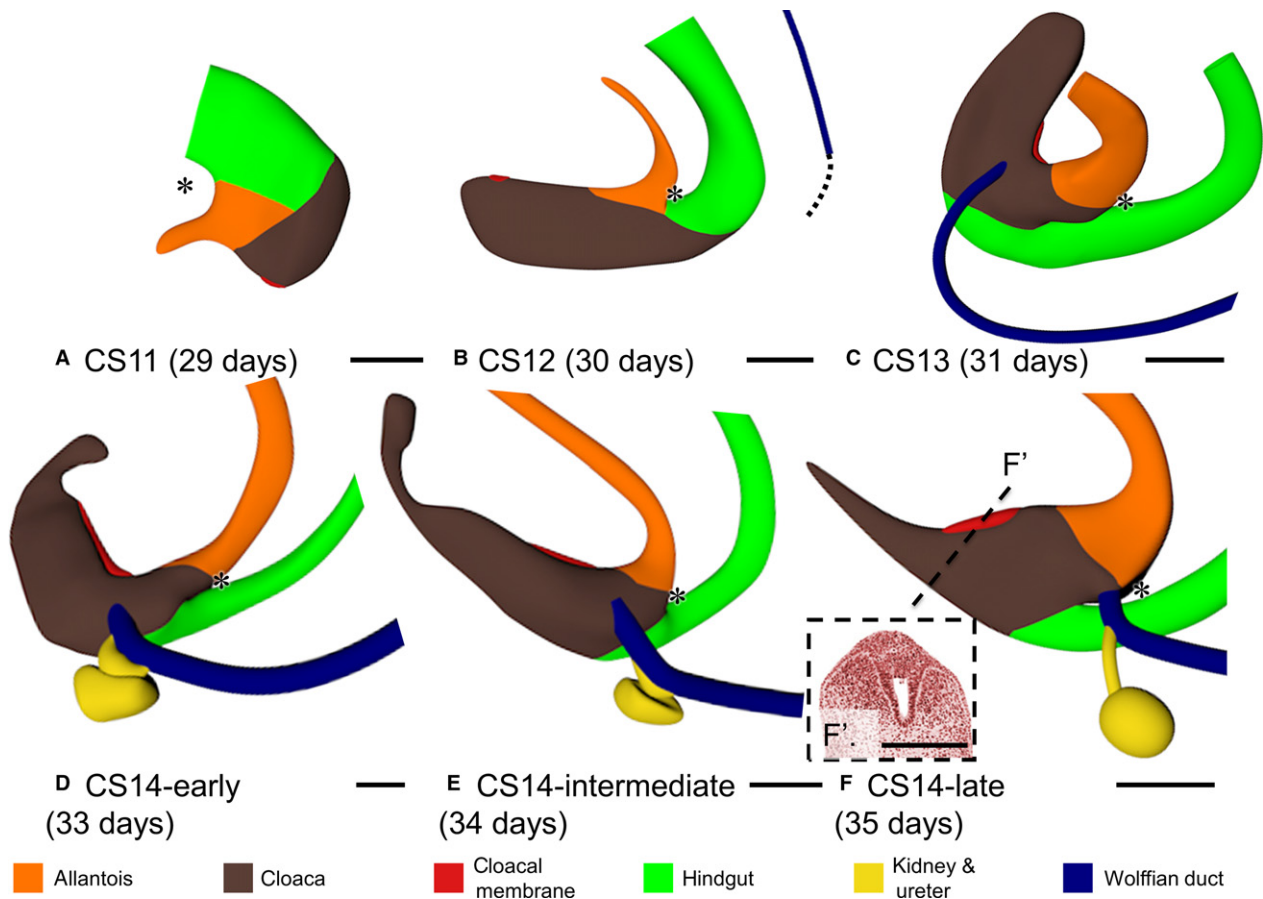
Fig. 2 Early phase of development of the cloacal region CS11–CS14 (A–D). Left-sided views. Cloaca (brown) and cloacal membrane (red) elongated in this period. Caudal to the cloacal membrane, the so-called 'tailgut' was maximally developed at CS13 (C), narrowed during CS14 (D–F) and had disappeared at CS15 (Fig. 4a). Wolffian ducts (dark blue) appeared at CS12 (B) and extended caudally (dotted line in b) to insert into the cloaca at CS13 (C). From CS14-early onwards (D–F), ureters and kidneys (yellow) were formed dorsolaterally on the Wolffian ducts just upstream of its insertion into the cloaca. The lateral folds separated the cranial part of the cloaca from the hindgut (green) between CS13 and CS14 (C–F; cf. Fig. 3). Up to CS14-late, no urorectal septum was found because the peritoneal cavity extended up to the junction of hindgut and cloaca. Asterisks: most caudal part of peritoneal trough. Panel (F') shows the appearance of the urethral plate in the ventral part of the cloacal membrane. Scale bar: 200 μm.

individual vertebrae; (ii) the insertion of the Wolffian duct into the cloaca/urogenital sinus; (iii) the transition of epithelium between urogenital sinus (pseudostratified columnar) and allantois (low cuboidal); (iv) the transition of epithelium between urethral plate (stratified epithelium) and cloacal membrane (simple epithelium); (v) the caudal tip of the urorectal septum; (vi) the caudal (deepest) point of the peritoneal trough in the urorectal septum; (vii) the caudal end of the dense cuff of mesenchyme surrounding the hindgut; (viii) the distal (ventral-most) tip of the mesenchymal condensation in the genital tubercle; and (ix) the tail-fold. When the tail-fold was no longer identifiable (after CS20), we used the midpoint between the external anal sphincter and the caudal tip of the coccyx. The cloacal membrane was defined as the area where the basal membrane between endodermal and ectodermal epithelium could not be distinguished. The transition of the (ventral) urethral plate into the (dorsal) cloacal membrane proper marks the boundary of growing and non-growing parts of the cloaca. The caudal cone of the dense cuff of mesenchyme surrounding the hindgut is a marker of the caudal end of the hindgut epithelium during the stages we studied (van der Putte & Neeteson, 1983).

Results

Axial curvature of embryo

The caudal end of the embryo bent ventrally between CS11 and CS13, and straightened again between CS14 and CS23. We determined the time course of this process by establishing the position of the C1, T1, L1, S1 and S5 vertebrae, and marking their centre on the notochord, which is an unambiguous and, therefore, reliable midline structure. Next, the angles determined by C1-T1-L1, T1-L1-S1 and L1-S1-S5 were measured. Vertebrae are still added caudally until CS14 (Fig. 1a–c; O'Rahilly & Müller, 2003). This extension results in a helical shape of the embryonic axis (Soffers et al. 2015). From CS14 onwards, the caudal region straightened (Fig. 1d–f). To confirm the unfolding process, C1-T1-L1, T1-L1-S5 and L1-S1-S5 angles were measured (Fig. 1g). Neck and thorax, as measured with the C1-T1-L1 angle,

Table 2 Average ages of CS (adapted from O'Rahilly & Müller, 2010).

CS	Ages (days)
10	28
11	29
12	30
13	31
14-early*	33
14-intermediate*	34
14-late*	35
15	36
16	39
17	41
18-early	43
18-late	45
20	49
23	56
9 weeks	63
10 weeks	70

*We subdivided CS14 into early, intermediate and late because of rapid developmental changes during this stage.

straightened slightly, but the lumbar (T1-L1-S5) and, in particular, the sacral region (L1-S1-S5) straightened in a more pronounced fashion between 4.5 and 6 weeks (CS14–CS17). After 6 weeks, only the L1-S1-S5 angle continued to increase (Fig. 1h), which corresponds with the development of the promontory (the lumbar lordosis only develops after birth; Reichmann & Lewin, 1971).

Shape of the developing cloaca

The cloaca connects to both allantois and hindgut. As the caudal end of the embryo folded and unfolded, the cloaca changed its shape (Fig. 2). From CS12 onwards the boundary of cloaca and allantois was identifiable as the transition of pseudostratified columnar epithelium (cloaca) into low cuboidal epithelium (allantois; Fig. 3a–e). We defined the cloacal membrane as the area where a basal membrane could not be distinguished between the endo- and ectodermal epithelium. Concomitant with caudal folding, cloaca and cloacal membrane elongated. This expansion corresponded in time with the presence of the tailbud in the caudal-most part of the embryo, which suggested that the tailbud provided cells for cloacal growth. The Wolffian ducts also extended caudally and inserted into the cloaca at CS13 (Fig. 2b,c), coincident with the disappearance of the tailbud. Subsequently, the caudal end of the body, including the cloaca, started to unfold. Furthermore, the part of the cloaca distal to the cloacal membrane began to regress by narrowing into the so-called 'tailgut', a transient structure that could only be identified during CS14 and disappeared entirely during CS15 (Figs 2d–f and 4a). The junction of cloaca and hindgut became identifiable, because the

hindgut epithelium thickened and the ventrocranial part of the cloaca widened more rapidly than the dorsocaudal part of the cloaca and the hindgut in CS13 and CS14 embryos (Fig. 3). Because the junction of hindgut and cloaca came to resemble the obliquely connected spout of a watering can, a semilunar ridge defined the cranial part of their junction on the inside (asterisks in Fig. 3). We interpreted this semilunar ridge as the so-called 'lateral folds' of the cloaca in many early studies (Retterer, 1890; Reichel, 1893). Figure 3f gives a 3D impression of the lateral folds between cloaca and hindgut at CS14-intermediate, when they extend to the Wolffian ducts. The lateral folds were identifiable from CS13 (31 days) to CS14-late (35 days; Fig. 3), when the folds had just passed beyond the insertion of the Wolffian ducts into the cloaca (Fig. 2f) and were effacing during CS15 (36 days; Fig. 3a–f). While the lateral folds were recognisable, the peritoneal cavity ('trough') reached down to the separation between hindgut and cloaca (asterisks in Fig. 2), that is, to the lateral folds.

Starting in CS15 embryos, a transverse wedge of loose connective tissue extended distally that further separated the cloaca into a larger ventral component, the urogenital sinus, and a smaller dorsal component, the future anal pecten region (Fig. 4). This wedge of loose connective tissue, which is known as the 'urorectal septum', only became recognisable after the lateral folds had separated the cloaca from the hindgut to just distal of the insertion of the Wolffian ducts (Fig. 2f). The insertion of the Wolffian ducts into the cloaca was a reliable landmark because it remained associated with segmental level 31–32 (S3–S4; Fig. 5b). This landmark revealed that the apparent cranial migration of the entrance of the Wolffian ducts into the cloaca and, later, the urogenital sinus was caused by a lack of growth of the cranial portion of the urogenital sinus between the entrance of the Wolffian ducts and the junction with the allantois (Fig. 5c). The peritoneal trough inside the urorectal septum (asterisks in Figs 2 and 4) extended caudally from just distal to the entrance of the Wolffian ducts at 36 days (CS15) to halfway the distance between the entrance of the Wolffian ducts and the caudal tip of the urorectal septum at 41 days (CS17) and back again in the next 2 weeks (Fig. 4).

Our description implies that the growth pattern of the cloacal region is complex. For that reason, we carried out measurements in our Amira reconstructions (Fig. 5). The distance between the entrance of the Wolffian duct and the middle of the cloacal membrane (Fig. 5c) increased linearly with time at ~10-fold the rate of the distance between the entrance of the Wolffian duct and the allantois. Because the Wolffian duct enters the cloaca near its centre at CS13 (Fig. 2c), these measurements show that growth primarily occurred in the caudal part of the cloacal region. Taking into account the shorter path, the distance between the entrance of the Wolffian duct and the caudal tip of the urorectal septum increased at a similar rate as that to
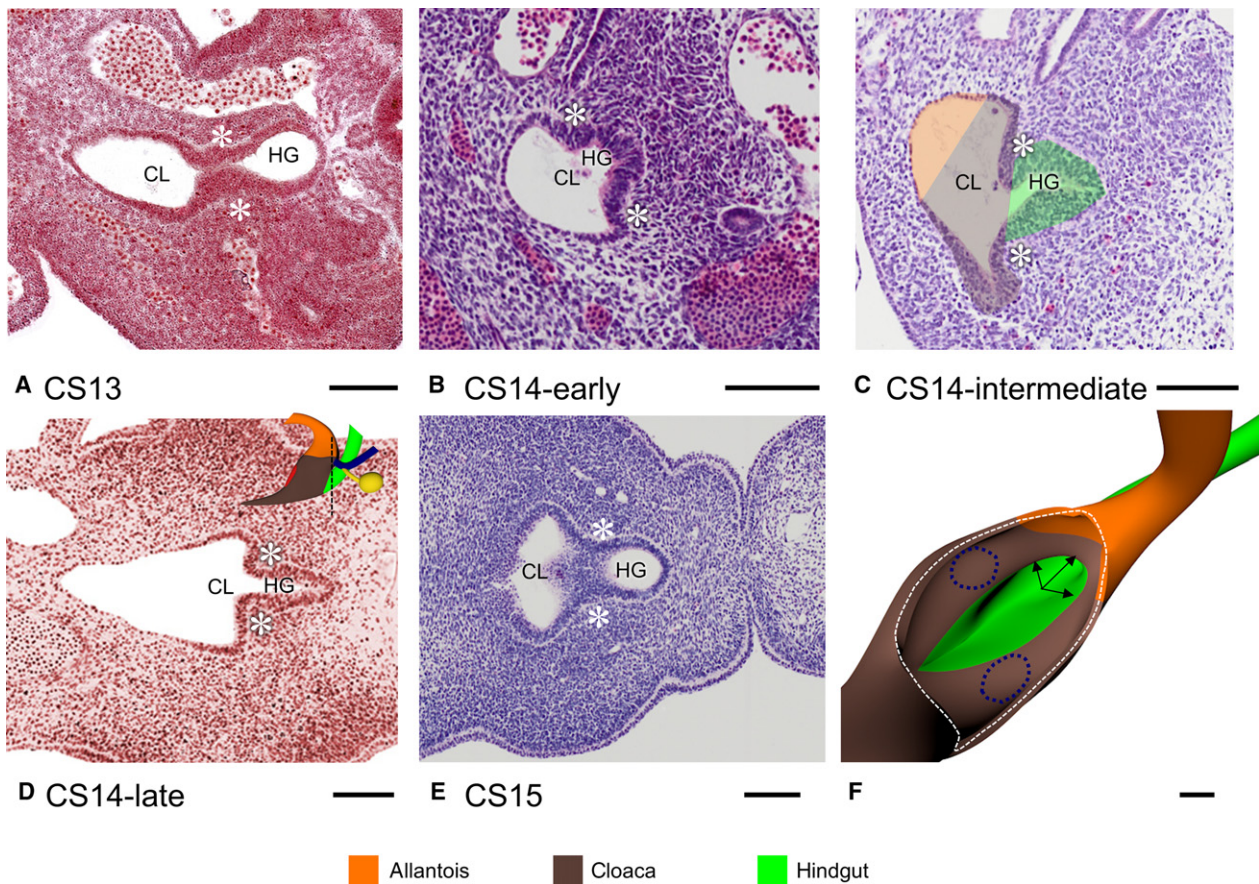
Fig. 3 The lateral fold. The lateral folds (asterisks) demarcate the junction between the dorso-cranial part of the cloaca and hindgut between CS13 and CS14-late. Note that the folds are first identifiable as blunt ridges at CS13 (A) to become pronounced ridges that demarcate the transition between the narrow hindgut and the wide cloaca (B–D) and efface again in CS15 (E). Panel (F) shows a 3D perspective of the sharp-edged lateral folds at CS14-intermediate (arrows) between cloaca (brown) and hindgut (green) of the embryo shown in (C). The position of the entrance of the Wolffian ducts is shown as dark blue dotted lines. CL, cloaca; HG, hindgut. Scale bar: 100 μm.

the cloacal membrane (Fig. 5d). The distance between the entrance of the Wolffian duct and the peritoneal trough first decreased (up to ~45 days or CS18) and then increased again (after 49 days CS20; Fig. 5d). This complex growth pattern is described qualitatively in the previous paragraph and can be traced in Figs 2 and 4 by following the position of the asterisks. The distance between the caudal tip of the urorectal septum and the ventral tip of the urethral plate increased exponentially at the same rate as the embryonic body at large (Fig. 5e). In contrast, the distance between the caudal tip of the urorectal septum and the dorsal end of the cloacal membrane decreased (Fig. 5e), which reveals a large and distinct growth difference between the ventral and dorsal parts of the cloaca. Similarly, the distance between the caudal tip of the urorectal septum and the tail-fold did not increase until after 39 days. Thereafter, this distance increased exponentially like that to the ventral tip of the urethral plate, but with a ~1-week delay. The area of restricted growth in the cloaca, therefore, seems strictly limited to the dorsal cloaca. To confirm these data, we also determined the distance between segment 32 (S5) and the ventral tip of the cloaca on the one hand (exponential growth at a slightly higher rate than the embryonic body at large) and the caudal tip of the urorectal septum on the other hand (also exponential growth; Fig. 5f), indicating that the growth of the vertebral column was not affected. In aggregate, these measurements show a more extensive growth in the caudal than cranial part of the cloaca, and a much more extensive growth in the ventral than dorsal part. The area of highest growth is the genital tubercle. This tubercle becomes identifiable at CS14-late, is similar in shape at CS18 and CS20, but has clearly changed in shape by CS23 (Fig. 6).

Ventral and dorsal parts of cloacal membrane

At the end of the 4th week (CS11 and CS12), the cloacal membrane was a thin, more or less circular structure on the ventral surface of the cloaca (Fig. 2a). As the caudal end of the body curved (CS13 and CS14), the cloacal
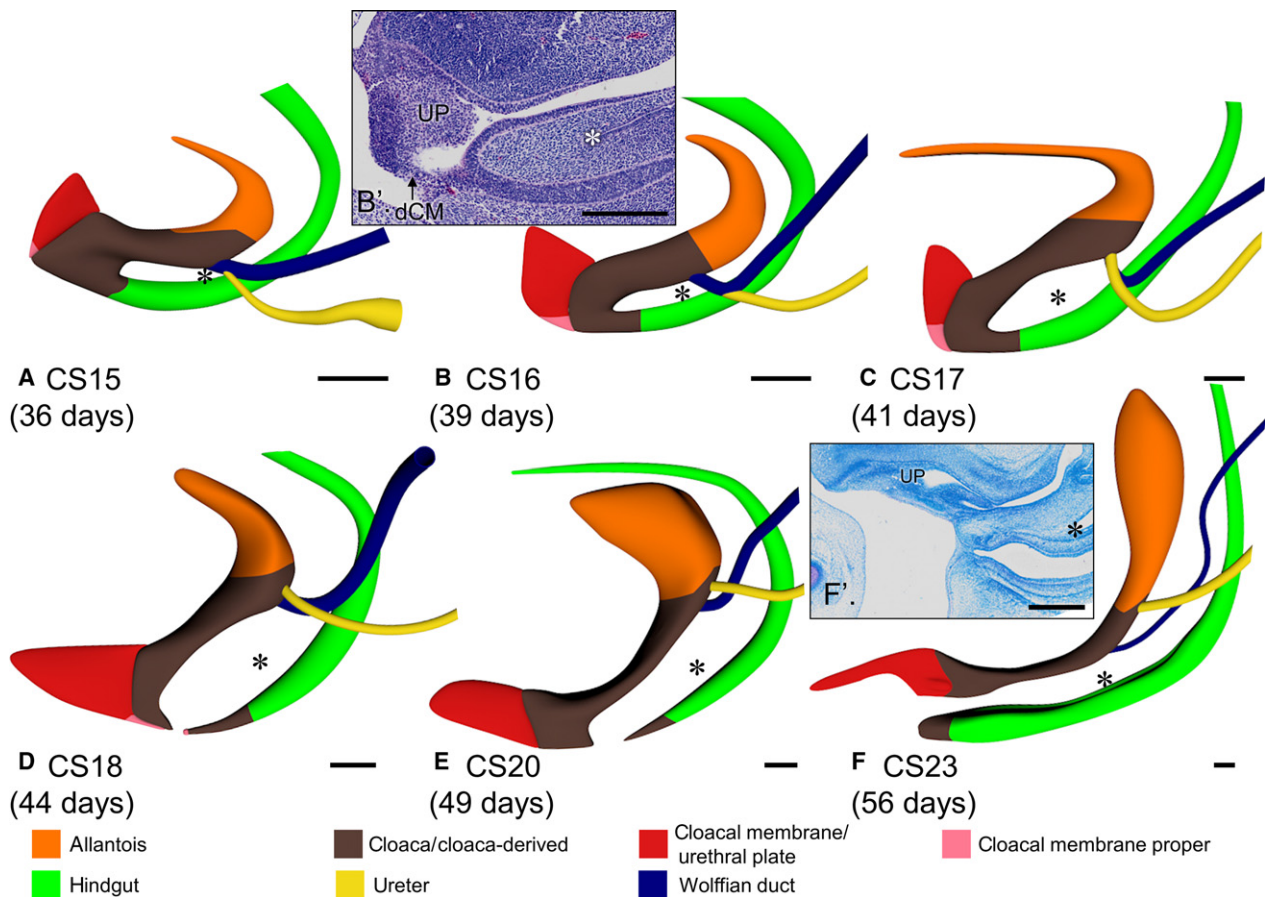
Fig. 4 Late phase of development of the cloacal region (CS15–CS23). Left-sided views aligned with respect to the caudal portion of the vertebral column. The cloaca resembled a U-shaped tube (A–C) with ventral urogenital and dorsal anorectal parts between CS15 and CS17, and the urorectal septum separating both parts. The urorectal septum consisted of loose mesenchyme (B′ and F′). The caudal-most point of the peritoneal trough in its centre is indicated with asterisks. Note that the caudal tip of the urorectal septum and the peritoneal trough move caudally relative to the Wolffian ducts (A–E; cf. Fig. 5b,d). The cloacal membrane consisted of a well-developed ventral urethral plate (UP; red) and a thin dorsal cloacal membrane proper (dCM; pink). The cloacal membrane proper did not grow between CS15 and CS17 (A–C), and ruptured at CS18 (D). Note the changing position of the cloaca due to the unfolding of the caudal body axis in (A–D) and its subsequent ventral extension concomitant with the growth of the genital tubercle (D–F). Scale bar: 200 μm.

membrane elongated and divided into a ventral part that proliferated to form a solid epithelial mass, the so-called 'urethral plate' (Figs 2f′ and 4b′,f′; UP), and a thin dorsal part that represented the cloacal membrane proper (Fig. 4b′; dCM). The apical part of the urethral plate was transiently covered on its caudal side with an ectodermal 'epithelial tag' (Fig. S6; van der Putte, 2004). Both parts of the cloacal membrane and the epithelial tag elongated between CS15 and CS17 (Fig. 4a–c). After CS18, the urethral plate continued to elongate, whereas the cloacal membrane proper did not grow and ruptured, starting at its centre at CS18 (Fig. 4d–f). Similarly, the epithelial tag on the urethral plate regressed towards the apex of the tubercle between CS17 and CS20, and had disappeared at CS23. In the reconstructions, the epithelial tag is visible as the epithelial cover of the urethral plate (Fig. S6). Only the growth of the urethral plate, therefore, mirrored that of the genital tubercle.

Mesenchymal component in the cloacal region

The developmental changes in the distribution of dense and loose mesenchyme in the cloacal region are incompletely described. Dense mesenchyme included PCM (blue code) and hindgut mesenchyme (HGM; green code; Fig. 7a), while loose mesenchyme occupied the remaining parts of the cloacal region, including the urorectal septum (Fig. 7a). Dense PCM became identifiable on the sides of the cloaca in CS14-late embryos (Fig. 7b). The bilateral PCMs expanded on the dorsocranial side of the urethral plate to form a single U-shaped 'roof' on the cranial side of the genital tubercle at CS15 (Fig. 7c). This PCM had also extended dorsally around the dorsal cloaca at CS20 (Fig. 7e). A separate cuff of dense mesenchyme with a tapering end at the junction of hindgut and cloaca surrounded the hindgut in embryos older than 5 weeks (CS15; Fig. 7b–f). Initially both areas of dense mesenchyme touched (CS15 and CS16; Fig. 7c), but as
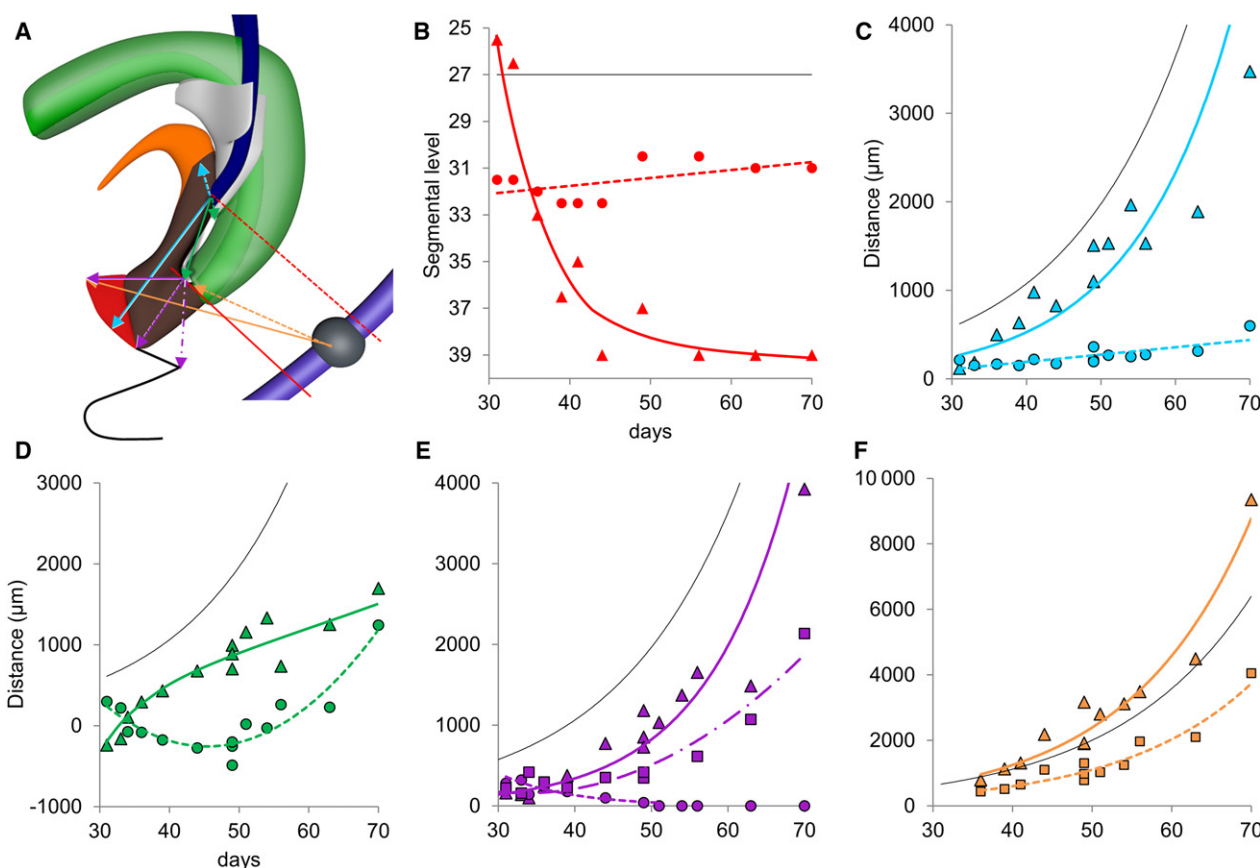
Fig. 5 Regional growth differences in the cloacal region. Panel (A) shows the landmarks used to prepare (B–F). Colours correspond to those in the respective graphs. The black line shows the position of the aortic bifurcation (b; Hikspoors et al. 2015) or the temporal changes in greatest length of the embryo (divided by 10; C–F; O'Rahilly & Müller, 2010). Panel (B) shows that the entrance of the Wolffian duct into the cloaca/urogenital sinus (dotted red line; R^2: 0.31) remained associated with segment 31–32 (S3–S4), whereas the tip of the urorectal septum (drawn red line; R^2: 0.87) moved caudally to the level of the last coccygeal vertebra. Panels (C) and (D) show the cranio-caudal growth of the cloacal region. The dotted blue line in (C) (R^2: 0.62) shows the marginal increase in distance between the entrance of the Wolffian duct and the allantois, whereas the distance between the entrance of the Wolffian duct and the middle of the cloacal membrane (continuous blue line; R^2: 0.82) grew at a similar rate as the body at large (black line). The continuous green line in (D) (R^2: 0.90) shows that the caudal tip of the urorectal septum moved from above (negative values) to below (positive values) the entrance of the Wolffian duct between 30 and 40 days. The distance then increased more slowly. The dotted green line (R^2: 0.88) represents the distance between the entrance of the Wolffian duct and the peritoneal trough. The biphasic shape of this measurement with an inflection at 50 days can also be deduced from the position of the asterisks in Figs 2 and 4. Panels (E) and (F) show the dorso-ventral growth of the cloacal region. The dotted purple line in (E) (R^2: 0.23) shows that the distance between the caudal tip of the urorectal septum and the cloacal membrane proper gradually declined, whereas the distance between the tip of the septum and the ventral tip of the urethral plate (drawn purple line; R^2: 0.90) increased concomitant with the growth rate of the embryo. The dash-dotted purple line in (E) (R^2: 0.92) shows that the distance between the tip of the septum and the tail-fold also increased, but with a delay of ~7 days (after CS20, the middle of the distance between the coccygeal tip and the anal sphincter was used instead of the tail-fold). Panel (F) shows the distances between the centre of S5 and the caudal limit of the hindgut mesenchyme (dotted orange line; R^2: 0.91) or the ventral tip of the mesenchyme of the genital tubercle (drawn orange line; R^2: 0.93). Both distances increase at a similar rate. Together with the dash-dotted line in (E), these data show that the absence of growth in the dorsal cloaca is a very local phenomenon. To demonstrate that growth was exponential some of the curves are shown in Fig. S2 after logarithmic transformation of the Y-axis.

the urorectal septum extended caudally, both areas became separated (CS18; Fig. 7d,g), showing that the loose mesenchyme of the urorectal septum was not solely a midline structure, but also extended laterally. Because the PCM expanded dorsally to embrace the anorectal part of the cloaca in the 8th week (CS20–CS23; Fig. 7e,f,h,i), PCM and HGM again became contiguous structures (Fig. 7f). At the same time, a shelf of dense mesenchyme, which formed in

the ventral-most part of the urorectal septum (Fig. 7h), began to expand ventrally between the surface ectoderm and the remaining part of the urethral plate (cf. Fig. 6e,f, with appearance of surface epithelium on developing perineum in Fig. 6f). At CS23, this structure could be identified as the spongious body (Fig. 7i). At this stage the other components of the PCM became identifiable as separate anatomical structures (external anal sphincter and
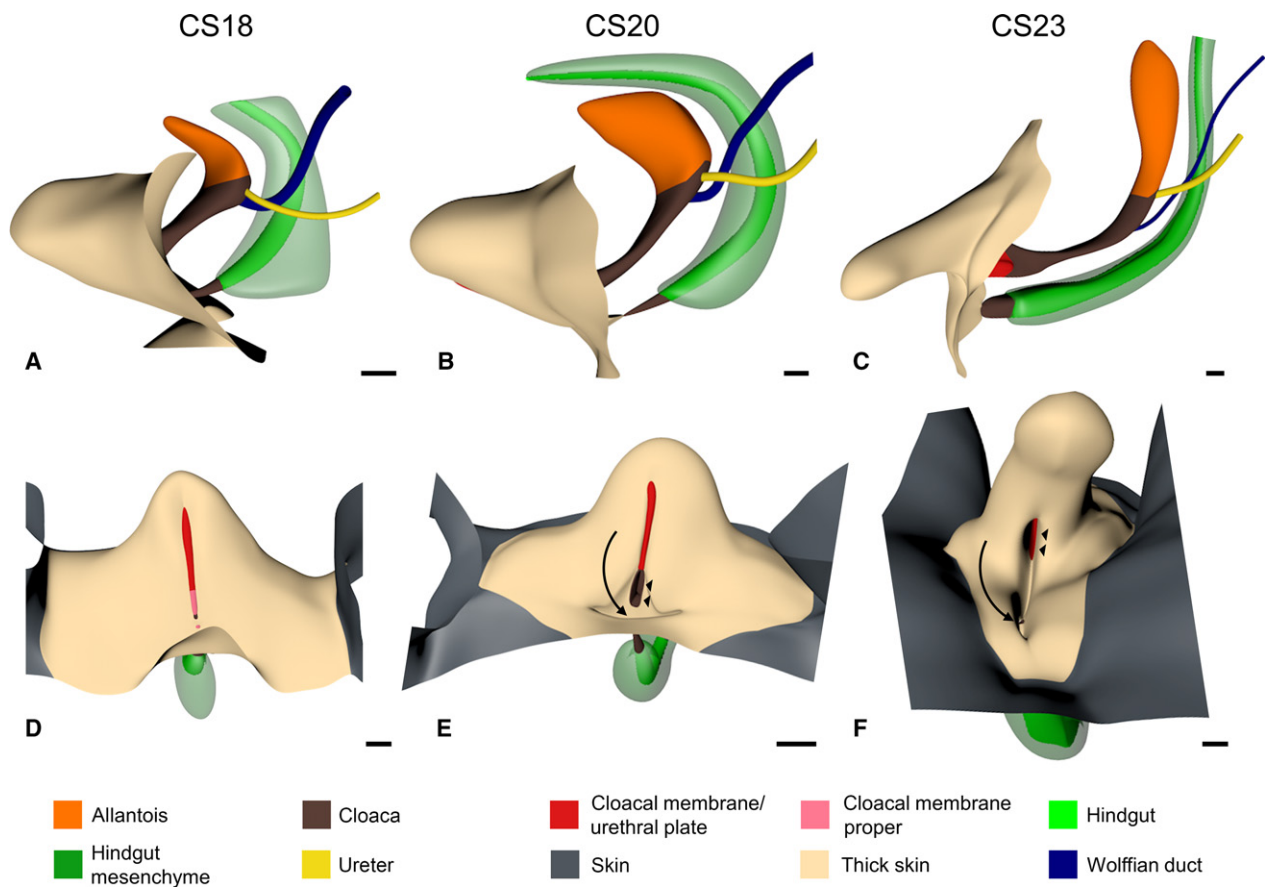
Fig. 6 The ectodermal cover of the cloacal region. Panels (A–C) show left-sided views and (D–F) frontal views of CS18, CS20 and CS23 embryos, respectively. The shape of the genital tubercle was similar at CS18 (A and D) and CS20 (B and E), but had changed at CS23 (C and F). The epithelium that covered the external genitals (sand-coloured) was markedly thicker than the more peripheral skin (dark grey). Further, note that a surface groove started to develop at CS20 (B and E) at the site of the ruptured cloacal membrane, which extended ventrally and became deeper in CS23 (C and F). The bottom of the groove in (E) and (F) contained the very narrow anorectal opening dorsally (arrow) and the wide urogenital opening ventrally (arrowheads). Scale bar: 200 μm.

bulbospongious muscle, cavernous body, ischiocavernous muscle, and urethral sphincter; Fig. 7i).

Development of the cranial part of the urogenital sinus and allantois

The portion of the urogenital sinus cranial to the entrance of the Wolffian ducts grew much slower than the caudal portion. The allantois remained a tubular structure until it started to balloon at CS20 (7 weeks). Shortly after the Wolffian ducts inserted into the cloaca at CS13, the ureteric buds started to form on the dorsal side of the Wolffian ducts near their insertion into the cloaca (Figs 2d–f and 3a,b). The portion of the Wolffian ducts between the cloaca and the ureteric buds disappeared at CS17 (41 days), so that both ureters gained access to the urogenital sinus as well (Fig. 4c). The entrance of the ureters into the urogenital sinus was first localised laterally (CS17) and gradually also cranially to the entrance of the Wolffian ducts, but remained within the domain of the epithelium of the cranial portion of the urogenital sinus. The insertions of the Wolffian ducts and ureters demarcate the trigone of the bladder (Fig. 3d–f).

Development of the anorectum

After the cloacal membrane ruptured at CS18, the cone-shaped small dorsal part of the cloaca retained only a very narrow opening to the outside. From CS20 onwards, this opening connected with the funnel-like ectodermal structure known as the 'anal pit'. In all our embryos, the connection was patent. The anorectum, therefore, derived from three different regions: the caudal hindgut, the dorsal cloaca and the anal pit (Fig. 6e,f). Up to CS15, the hindgut connected to the dorsal side of the cloaca forming the lateral folds as described above. After CS15, the hindgut only connected to the dorsal part of the cloaca. The boundary of hindgut and cloaca was marked by the distal end of the
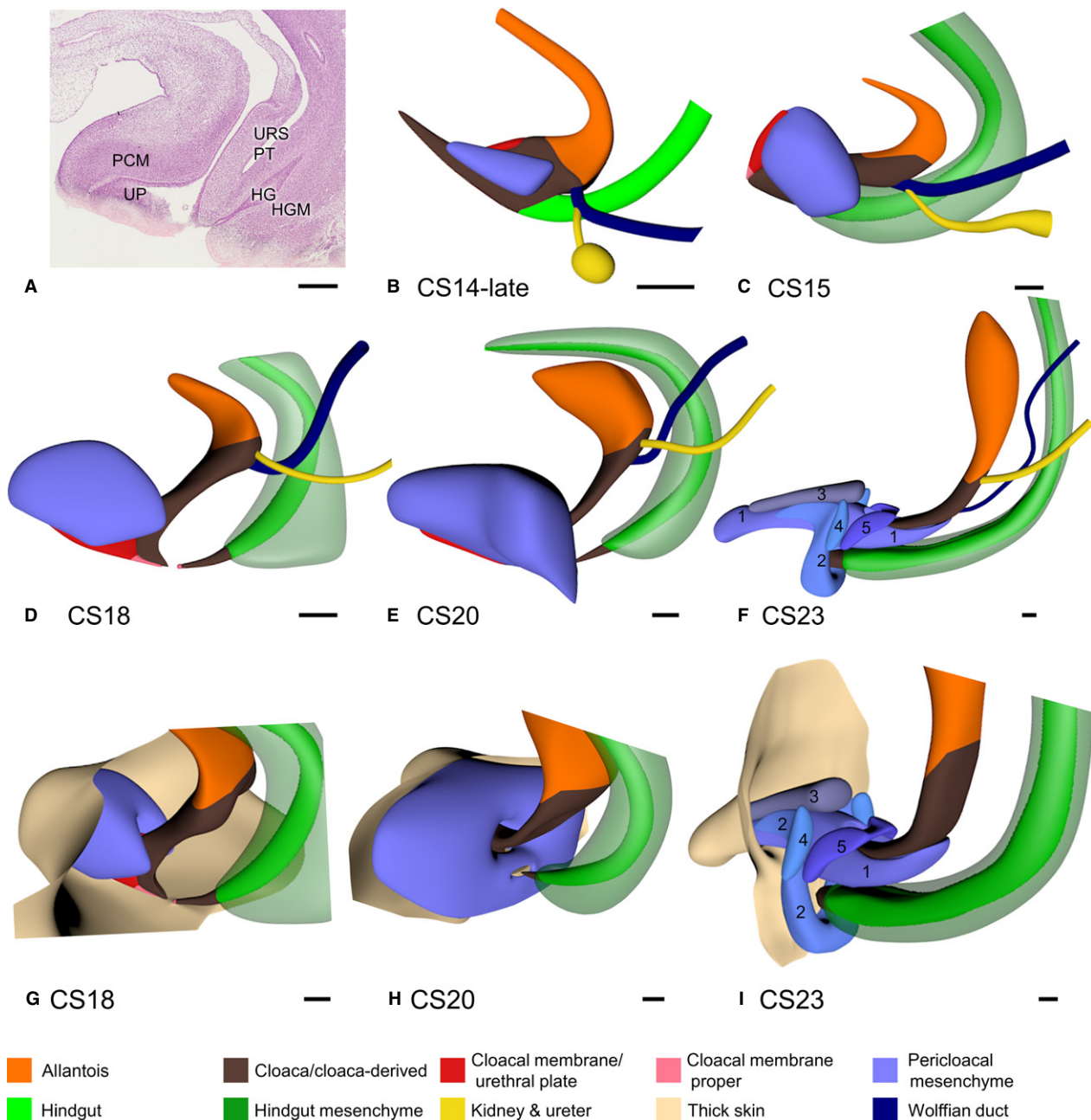
Fig. 7 Growth of mesenchymal masses in the cloacal region. Panel (A) shows a sagittal section of the cloacal region of a CS20 embryo to show the differences between dense [e.g. the pericloacal mesenchyme (PCM)] and loose connective tissue [e.g. urorectal septum (URS)]. Panels (B–F) show the 3D shape and location of the PCM (blue) and the hindgut mesenchyme (HGM; green) between CS14-late and CS23 (33–56 days). The PCM was first identifiable on both sides of the cloaca at CS14-late, extended ventrally and cranially to embrace the cranial side of the cloaca between CS15 and CS18, and extended dorsally embracing the caudal-most part of the cloaca after CS20. At CS23 (F and I), the components of the PCM had become identifiable: spongious body (1), external anal sphincter and bulbospongious muscle (2), cavernous body (3), ischiocavernous muscle (4), and urethral sphincter (5). The caudal end of the HGM coincided with the junction of hindgut (green) and cloaca (brown) from CS15 onwards (C–F; transparent green). HG, hindgut; HGM, hindgut mesenchyme; PCM, pericloacal mesenchyme; PT, peritoneal trough; UP, urethral plate. Scale bar: 200 μm.

dense mesenchymal cuff (HGM) that surrounded the hindgut (Fig. 7). The junction of dorsal cloaca and anal pit is characterised by the transition from pseudostratified to stratified squamous epithelium (Figs 4f′ and S3).

Discussion

We studied the development of the cloacal region to clarify the mechanism of cloacal subdivision and the fate of cloacal

derivatives (Figs S4–S6). A pronounced difference in growth between the rapidly growing ventral and central areas, and the hardly growing cranial and dorsal areas produced separate urogenital and anorectal compartments in the cloacal lumen (Fig. 8). Regressive development of the dorsal cloaca transformed the 'end-to-end' connection of the hindgut and cloaca into an 'end-to-side' connection during CS13 and CS14, with the lateral folds marking the junction of cloaca and hindgut during this transformation. The dorsoventral difference in growth subsequently straightened the curved caudal body axis of the embryo and concomitantly extended the urorectal septum caudally. The subdivision of the cloacal membrane into a rapidly growing, thick urethral plate ventrally and a hardly growing, very thin membrane dorsally best represented the dorsoventral difference in growth. The cloacal membrane proper ruptured at CS18.

Mechanism of cloacal subdivision

The mechanism of cloacal subdivision has remained controversial with respect to origin and growth of the septum that separates its ventral urogenital and dorsal anorectal parts. Early studies emphasized the role of the lateral ('Rathke's') folds (Retterer, 1890; Reichel, 1893) or the frontal urorectal ('Tourneux's') septum (Tourneux, 1888). Unfortunately, the descriptions of the shape of the lateral folds and timing of the developmental appearance of folds and urorectal septum were sufficiently diffuse to induce textbook writers to combine both concepts (Carlson, 2014; Schoenwolf et al. 2015; Moore et al. 2016). Our present study, therefore, defined the lateral folds and showed that their temporary presence marks a changing attachment of the hindgut to the cloaca. When the cloaca forms between 28 and 30 days (CS10–CS12), it is a smooth, caudal extension of the hindgut with an 'end-to-end' type of junction. During the next few days (CS13–CS14-late), this connection transformed into an 'end-to-side' type of junction and its position changed from cranial to dorsal relative to the cloaca (Kluth et al. 1995, fig. 2). We consider this change in position of the connection of hindgut and cloaca as the first sign of dorsal cloacal regression.

The dorsoventral difference in growth of cloaca and surrounding mesenchyme has also been associated with the caudal extension of the urorectal septum (van der Putte, 2004; Huang et al. 2016). The combination of lengthening of the body axis with an increasingly convex curvature (Müller & O'Rahilly, 2004) suggests an initial predominance of dorsal growth (for the consequence of insufficient dorsal growth at this stage, see van de Ven et al. 2011). However, the subsequent uncurling of the body axis in the 6th week (CS14–CS18; Paidas et al. 1999) indicates a change to predominantly ventral growth. This regional change in growth is important, because some claim that the urorectal septum actively descends caudally ('active' theory; Pohlman, 1911;

Stephens, 1988), whereas others consider the growth of the urorectal septum and, hence, the septation of the cloaca as merely the result of the differential dorsoventral growth in the cloacal region ('passive' theory; van der Putte, 2004; Xu et al. 2012; Tschopp et al. 2014; Matsumaru et al. 2015; Huang et al. 2016). To distinguish between both conjectures, the entrance of the Wolffian ducts into the cloaca/urogenital sinus is a reliable landmark, because its position is fixed to segments 31–32 (vertebrae S3–S4). Our measurements (Fig. 5) show that the cranial and dorsal areas of the cloaca hardly grow, whereas the ventrocaudal area, including the surrounding cloacal mesenchyme, grows at a similar rate as the embryo at large. Our measurements in human embryos, therefore, support the passive theory. Other convincing non-quantitative arguments in favour of pronounced regional growth differences in the cloaca are disappearance of the tailgut, apoptosis in the dorsal cloaca, absence of growth of the dorsal cloacal membrane, and pronounced growth of the ventral part of the cloacal membrane (urethral plate; van der Putte, 1986, 2004; Nievelstein et al. 1998; Sasaki et al. 2004; Matsumaru et al. 2015). Furthermore, the urorectal septum consists of loose rather than dense mesenchyme that one usually associates with local cell proliferation.

Fate of the cloaca

The topographic distribution of the regional differences in growth rate of the cloaca determines the remodelling of the cloaca. Figure 8 shows that the rapidly growing central part of the cloaca is initially sandwiched between slowly growing cranial (future vesical trigone) and dorsal parts (future anal pecten). As a result, the Wolffian ducts appear to move cranially and dorsally on the surface of the cloaca, as was earlier observed in mice (Matsumaru et al. 2015). Similarly, the anorectal part of the cloaca becomes a progressively smaller part due to the difference in growth of the dorsal and ventral parts of the cloaca.

Cell replication rates in the cloacal wall and its surrounding mesenchyme appear similar in human (Nebot-Cegarra et al. 2005) and mouse embryos (Matsumaru et al. 2015), but rapid proliferation may continue longer in mesenchyme than epithelium (Matsumaru et al. 2015). Observed regional differences in growth, therefore, point to regional accumulation of extracellular matrix or regional differences in cell death. In early mouse embryos (up to CS14), apoptosis in the cloacal epithelium is prevalent ventrally and dorsally, with an almost apoptosis-free area in the centre, while apoptosis in the surrounding mesenchyme concentrates around the anorectal part of the cloaca. Thereafter, apoptosis is mainly seen in the mesenchyme of the urorectal septum caudal to the Wolffian ducts (Sasaki et al. 2004; Batourina et al. 2005; Matsumaru et al. 2015), the epithelium of the caudal tip of the urorectal septum and the dorsal part of the cloacal membrane (Ng et al. 2014).
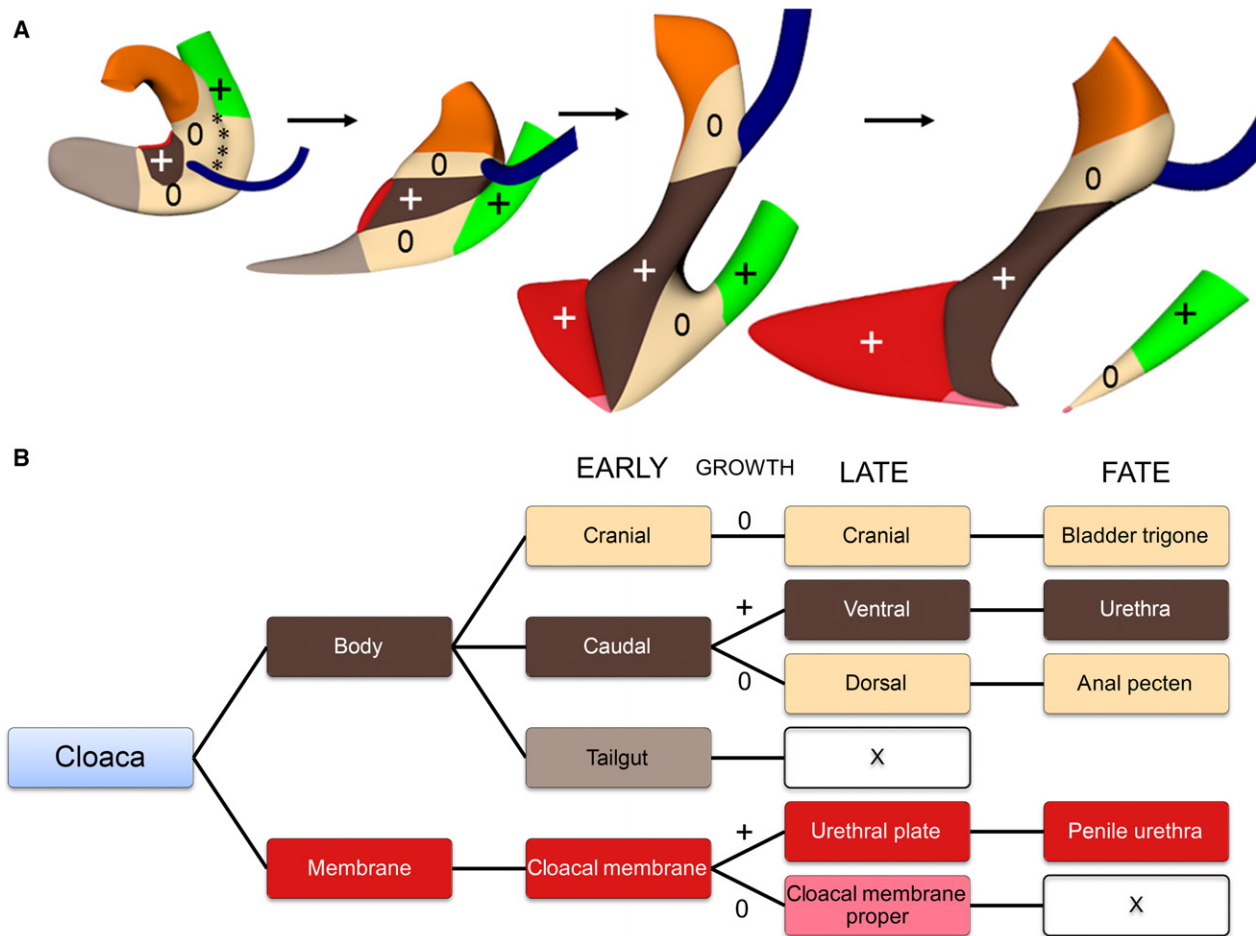
Fig. 8 Proposed mechanism of cloacal subdivision and the fate of the cloaca. Panel (A) shows the global distribution of 'growing' and 'non-growing' zones in the cloaca of CS13, CS14-late, CS15 and CS18 embryos. Initially, the non-growing zone is located in the cranial and dorsal portions of the cloaca and surrounds the ventral (central) growing zone. Growth in the ventral portion changes the shape of the cloaca and eventually mediates the separation into urogenital and anal compartments. Panel (B) shows the fate of the cloaca in three phases: early (CS11–14), late (CS15–18) and definitive (fate). The colour codes in (A) and (B) correspond. Symbols: +, growing; 0, non-growing; X, disappear.

Fate of cloacal membrane and pericloacal mesenchyme

The ventrocaudal part of the cloaca, including the ventral part of the cloacal membrane and the PCM, represents the expanding part in the cloacal region. Concomitant with the ventral expansion of the genital tubercle, the length of the cloacal membrane increases during CS14 (33–35 days; Fig. 2). The expanding and non-expanding parts of the cloacal membrane can be distinguished in sections and reconstructions from CS15 onwards, when the ventral part of the membrane not only increases in length, but also in height (Fig. 4; Ludwig, 1965; Penington & Hutson, 2002b; Hynes & Fraher, 2004; Li et al. 2015), with most of the epithelium being endodermal (van der Putte, 2004; Seifert et al. 2008). Due to the expansion of the urethral plate, the connection between the relatively wide lumen of the lower urogenital sinus and the part of the cloacal lumen overlying the thin dorsal part of the cloacal membrane is narrow and known as the 'cloacal duct' (Felix, 1912, fig. 650). The centre

of the thin cloacal membrane ruptures at CS18 (44 days), with often a dorsal remnant ('anal membrane') temporarily covering the anorectal outlet remaining (Ludwig, 1965; Nievelstein et al. 1998). Growth of the PCM depends on Sonic Hedgehog secretion by the endodermal cloacal epithelium (Haraguchi et al. 2007; Lin et al. 2009; Seifert et al. 2009). Dense masses of PCM become identifiable bilaterally of the cloaca at CS14-late (35 days), expand cranially to bridge the urethral plate (at CS18; 44 days), and then dorsally to surround urogenital sinus (CS20; 49 days), anorectal junction and anal pit (CS23; 56 days). The portion of the dense PCM between urogenital sinus and anorectal junction began to expand ventrally in the 8th week to form the penile urethra (Seifert et al. 2009).

Fate of the dorsal cloaca

The dorsal part of cloaca, including the dorsal cloacal membrane, is, in contrast, a 'non-growing' area (Fig. 5e; van der

Putte, 1986, 2004; Huang et al. 2016). The decline is visible qualitatively: the narrowing tailgut impresses as a transient stage in the regression of the dorsocaudal cloaca during CS14 (33–35 days), the dorsal cloacal membrane proper thins and ruptures after CS18 (44 days), and the dorsal cloaca (developing anal pecten) becomes a narrow, cone-shaped structure with a very small opening between CS17 and CS20 (41–49 days; Fig. 4) without any dense PCM surrounding it until CS20 (49 days; Fig. 7; van der Putte, 1986). Microscopically, the dorsocaudal area is characterised by a high prevalence of apoptotic cells between CS14 and CS20 (~34–49 days; Sasaki et al. 2004; Ng et al. 2014; Matsumaru et al. 2015). Interestingly, the area affected by the lack of growth is also limited dorsally: the area of the tail-fold does not grow up to CS18 (41 days; Fig. 5e), but thereafter the (pre-)vertebral sacral and coccygeal tissues exhibit a similar growth rate as the ventral part of the cloaca (Fig. 5e,f). The hindgut and its surrounding dense mesenchymal cuff, the future smooth-muscle layer of the rectum, also appear to expand normally (the caudal end of the mesenchymal cuff can serve as a reliable marker for junction between the hindgut and anorectal part of the cloaca; van der Putte & Neeteson, 1983). Until CS18 (44 days), the dense PCM flanks the urethral plate as urethral folds but, by expanding dorsally around the urogenital and anal openings during the next 2 weeks, these urethral folds and the groove they embrace merge with the perianal folds and anal pit (Fig. 4d–f). The endoderm of the hindgut and that of the dorsal cloaca, and the ectoderm of the anal pit are easily distinguishable in histological sections and 3D models thereof (Fritsch et al. 2007; Yamaguchi et al. 2008). These zones can be traced to the epithelium of the formed rectum (simple columnar epithelium), the anal pecten (non-keratinised stratified squamous epithelium) and the perianal skin (keratinised stratified squamous epithelium), respectively.

Development of bladder and trigone

Apoptosis in the epithelium of the distal Wolffian duct and cloaca is necessary for insertion of the Wolffian duct at CS13 (31 days; Hoshi et al. 2018), while apoptosis in the common nephric duct separates the entrance of the Wolffian duct and ureter into the urogenital sinus between CS15 and CS20 (36–49 days) to establish the vesical trigone (Batourina et al. 2005; Matsumaru et al. 2015). Further support for this mechanism comes from tissue-recombination experiments of trigonal epithelium and fetal urogenital-sinus mesenchyme in mice, which demonstrate that trigonal epithelium derives from urogenital endoderm and not from the mesodermal common nephric duct (Tanaka et al. 2010), while the Cre-lox genetic recombination technique has shown that the underlying smooth muscle forms from bladder smooth muscle (Viana et al. 2007). The bladder fundus develops from the intra-abdominal portion of the allantois (van der Putte, 2006; Georgas et al. 2015). The fundus

develops a muscular wall and begins to expand after the trigone has formed at CS20 (Fig. 4), and extends, flanked by both umbilical arteries, as an intraperitoneal structure up to the umbilical ring to transform into a retroperitoneal structure only after the 4th month (Cunéo & Veau, 1899).

Fate of the peritoneal trough

The position of the 'deepest' (most caudal) part of the peritoneal trough between urogenital sinus and hindgut first descended caudally after CS13 to touch the developing levator ani muscle at CS18 and CS20, and then ascended again to just caudal of the junction of the Wolffian ducts with the urogenital sinus (Figs 2, 4 and 5d). In rodents, the configuration as seen between CS18 and CS20 persists into adult life (Treuting & Dintzis, 2012; Navarro et al. 2017), so that the caudal boundary of the peritoneal trough in human CS18–CS20 embryos (and adult rodents) is apparently localised more caudally than in adult humans (~12 cm above the pelvic floor). The trough disappears due to a widening of the dorsal mesentery from caudal to cranial between CS20 and CS23 that is accompanied by an increase in the distance between the levator ani muscle and the deepest point of the trough (our unpublished observations). In fetuses of 9–10 weeks the deepest point of the prerectal peritoneal pouch is located in the plane through S3 and symphysis (Fritsch, 1988), that is, at the same location as in the adult. These topographic relations are also found between 22 and 35 weeks of fetal life (Saguintaah et al. 2002). The only structure that can explain the transition of the configuration at 6 weeks to that at 9–10 weeks is 'Denonvilliers' fascia'. Based on a single embryo, Cunéo & Veau (1899) first proposed that Denonvilliers' fascia developed from the obliterated peritoneal trough by adhesion and fusion of its peritoneal walls. Their model was subsequently vindicated (Tobin & Benjamin, 1945; Uhlenhuth et al. 1948). In agreement, pelvic surgeons occasionally report peritoneal troughs that extend to the pelvic floor in neonates (Uhlenhuth et al. 1948) or coelomic remnants on the pelvic floor in adults (Heald & Moran, 1998). The fascia as such develops only after birth (Kraima et al. 2015).

Implications for cloacal malformations

Cloacal malformations are still poorly understood, and classifications tend to emphasize anatomical or clinical rather than developmental aspects (Holschneider et al. 2005). Anorectal malformations are often associated with caudal regression. In rodents, deficiency of homeobox genes like Cdx family members and an excess of retinoic acid can, acting via inhibition of WNT signalling, both cause dosage-dependent caudal vertebral and urorectal defects (Padmanabhan, 1998; van de Ven et al. 2011). Deficiency in SHH signalling in the caudal endoderm causes, independently of CDX, dosage-dependent inhibition of cloacal development

(Mo et al. 2001). Interestingly, the dorsal (anorectal) part of the cloaca appears to be more sensitive to SHH deficiency than the ventral, urogenital part (Runck et al. 2014). The separate roles of the homeobox genes and SHH may explain the weak correspondence between the type of anorectal malformation and pelvic floor development in human anorectal malformations (Smith & Stephens, 1988; de Vries, 1988), and why striated pelvic floor muscles are nearly always present if development of the sacrum is not affected (Wilkinson, 1972).

We have identified differential growth of the ventral and dorsal parts of the cloaca as a prominent feature of normal development between 4.5 and 7 weeks of development. Its onset coincides with the switch from predominant growth in the dorsal part of the caudal embryo (resulting in the curling-up of the caudal body axis) to growth in the ventral part of the caudal embryo (resulting in straightening of the caudal body axis; Fig. 1). The near absent growth of the dorsal cloaca becomes manifest at CS14 with transformation of the caudal cloaca into the tailgut, continues with disappearance of the tailgut at CS15, and results in a similar size and shape of dorsal cloaca and cloacal membrane between CS15 and CS20, with the weak middle portion of the cloacal membrane normally rupturing at CS18 [the dorsal-most portion of the cloacal membrane proper persists temporarily as the 'anal membrane' (our observations in an CS18-early embryo; Fritsch et al. 2007; van der Putte, 2009)]. Too little or absent regressive development of the dorsal cloaca results in its persistence. This group of malformations is phenotypically characterised by more extensive development of the dorsal portion of the cloacal membrane proper (the portion corresponding to the anal membrane) and its surrounding mesenchyme so that, with increasing severity of the malformation of the anal opening, becomes positioned more ventrally on the perineum and then more cranially on the urogenital sinus (van der Putte & Neeteson, 1984; van der Putte, 1986, 2006). Due to the strengthening of the dorsal part of the cloacal membrane proper, the abnormally localised anal opening is smaller or does not form, but the musculature surrounding the anorectum follows its change in topographic position, at least in hereditary pig models (van der Putte & Neeteson, 1984; Lambrecht & Lierse, 1987). Too much regression of the dorsal cloaca leads, on the other hand, to stenosis or atresia of the anorectal junction (van der Putte, 1986; Nievelstein et al. 1998; Fritsch et al. 2007), and reportedly insufficient development of the internal anal sphincter (Fritsch et al. 2007).

Conclusion

The subdivision of the cloaca appears to be based on differential growth of the 'growing' ventral (central) and 'non-growing' craniodorsal parts of the cloacal region. The growing central zone is initially sandwiched between the non-growing zones, but eventually separates the urogenital and anorectal compartments and forms the genital tubercle.

Competing interests

The authors declare that they have no competing interests.

Author contributions

N.K. participated in data collection, analysis and visualisation, and wrote the manuscript. J.H. and H.M. participated in data analysis and interpretation. G.M. and N.K. were responsible for formatting all figures. K.M., W.W., S.A. and S.E.K. participated in data analysis and interpretation, provided guidance, and edited the manuscript. W.L. conceived the study, provided guidance and assisted with data interpretation, and helped in manuscript writing and editing.

References

Batourina E, Tsai S, Lambert S, et al. (2005) Apoptosis induced by vitamin A signaling is crucial for connecting the ureters to the bladder. *Nat Genet* **37**, 1082–1089.

Carlson BM (2014) *Human Embryology and Developmental Biology*. Philadelphia: Saunders-Elsevier.

Cunéo B, Veau V (1899) De la signification morphologique des aponévroses périvésicales. *J Anat Physiol* **35**, 235–245.

Felix W (1912) The development of the urinogenital organs. In: *Manual of Human Embryology*. (eds Keibel F, Mall FP), pp. 752–979. Philadelphia, PA: J.B. Lippincott.

Fritsch H (1988) Developmental changes in the retrorectal region of the human fetus. *Anat Embryol (Berl)* **177**, 513–522.

Fritsch H, Aigner F, Ludwikowski B, et al. (2007) Epithelial and muscular regionalization of the human developing anorectum. *Anat Rec (Hoboken)* **290**, 1449–1458.

Georgas KM, Armstrong J, Keast JR, et al. (2015) An illustrated anatomical ontology of the developing mouse lower urogenital tract. *Development* **142**, 1893–1908.

Haraguchi R, Motoyama J, Sasaki H, et al. (2007) Molecular analysis of coordinated bladder and urogenital organ formation by Hedgehog signaling. *Development* **134**, 525–533.

Heald RJ, Moran BJ (1998) Embryology and anatomy of the rectum. *Semin Surg Oncol* **15**, 66–71.

Hikspoors JP, Soffers JH, Mekonen HK, et al. (2015) Development of the human infrahepatic inferior caval and azygos venous systems. *J Anat* **226**, 113–125.

Holschneider A, Hutson J, Peña A, et al. (2005) Preliminary report on the International Conference for the Development

of Standards for the Treatment of Anorectal Malformations. *J Pediatr Surg* **40**, 1521–1526.

Hoshi M, Reginensi A, Joens MS, et al. (2018) Reciprocal spatiotemporally controlled apoptosis regulates Wolffian duct cloaca fusion. *J Am Soc Nephrol* **29**, 775–783.

Huang YC, Chen F, Li X (2016) Clarification of mammalian cloacal morphogenesis using high-resolution episcopic microscopy. *Dev Biol* **409**, 106–113.

Hynes PJ, Fraher JP (2004) The development of the male genitourinary system: II. The origin and formation of the urethral plate. *Br J Plast Surg* **57**, 112–121.

Ikebukuro K, Ohkawa H (1994) Three-dimensional analysis of anorectal embryology. *Pediatr Surg Int* **9**, 2–7.

Kluth D, Hillen M, Lambrecht W (1995) The principles of normal and abnormal hindgut development. *J Pediatr Surg* **30**, 1143–1147.

Kluth D, Fiegel HC, Geyer C, et al. (2011) Embryology of the distal urethra and external genitals. *Semin Pediatr Surg* **20**, 176–187.

Kraima AC, West NP, Treanor D, et al. (2015) Whole mount microscopic sections reveal that Denonvilliers' fascia is one entity and adherent to the mesorectal fascia; implications for the anterior plane in total mesorectal excision? *Eur J Surg Oncol* **41**, 738–745.

Lambrecht W, Lierse W (1987) The internal sphincter in anorectal malformations: morphologic investigations in neonatal pigs. *J Pediatr Surg* **22**, 1160–1168.

Li Y, Sinclair A, Cao M, et al. (2015) Canalization of the urethral plate precedes fusion of the urethral folds during male penile urethral development: the double zipper hypothesis. *J Urol* **193**, 1353–1360.

Lin C, Yin Y, Veith GM, et al. (2009) Temporal and spatial dissection of Shh signaling in genital tubercle development. *Development* **136**, 3959–3967.

Ludwig KS (1965) Über die Beziehungen der Kloakenmembran zum Septum urorectale bei menschlichen Embryonen von 9 bis 33 mm SSL. *Z Anat Entwicklungsgesch* **124**, 401–413.

Matsumaru D, Murashima A, Fukushima J, et al. (2015) Systematic stereoscopic analyses for cloacal development: the origin of anorectal malformations. *Sci Rep* **5**, 13 943.

Mo R, Kim JH, Zhang J, et al. (2001) Anorectal malformations caused by defects in Sonic Hedgehog signaling. *Am J Pathol* **159**, 765–774.

Moore KL, Persaud TV, Torchia MG (2016) *The Developing Human: Clinically Oriented Embryology*. Philadelphia, PA: Elsevier.

Müller F, O'Rahilly R (2004) The primitive streak, the caudal eminence and related structures in staged human embryos. *Cells Tissues Organs* **177**, 2–20.

Navarro M, Ruberte J, Carretero A, et al. (2017) Digestive tract. In: *Morphological Mouse Phenotyping: Anatomy, Histology and Imaging*. (eds Ruberte J, Carretero A, Navarro M), pp. 89–146. Amsterdam: Elsevier.

Nebot-Cegarra J, Fàbregas PJ, Sánchez-Pérez I (2005) Cellular proliferation in the urorectal septation complex of the human embryo at Carnegie stages 13–18: a nuclear area-based morphometric analysis. *J Anat* **207**, 353–364.

Ng RC, Matsumaru D, Ho AS, et al. (2014) Dysregulation of Wnt inhibitory factor 1 (Wif1) expression resulted in aberrant Wnt-beta-catenin signaling and cell death of the cloaca endoderm, and anorectal malformations. *Cell Death Differ* **21**, 978–989.

Nievelstein RA, Van Der Werff JF, Verbeek FJ, et al. (1998) Normal and abnormal embryonic development of the anorectum in human embryos. *Teratology* **57**, 70–78.

O'Rahilly R, Müller F (2003) Somites, spinal ganglia, and centra. *Cells Tissues Organs* **173**, 75–92.

O'Rahilly R, Müller F (2010) Developmental stages in human embryos: revised and new measurements. *Cells Tissues Organs* **192**, 73–84.

Padmanabhan R (1998) Retinoic acid-induced caudal regression syndrome in the mouse fetus. *Reprod Toxicol* **12**, 139–151.

Paidas CN, Morreale RF, Holoski KM, et al. (1999) Septation and differentiation of the embryonic human cloaca. *J Pediatr Surg* **34**, 877–884.

Penington EC, Hutson JM (2002a) The cloacal plate: the missing link in anorectal and urogenital development. *BJU Int* **89**, 726–732.

Penington EC, Hutson JM (2002b) The urethral plate – does it grow into the genital tubercle or within it? *BJU Int* **89**, 733–739.

Pohlman AG (1911) The development of the cloaca in human embryos. *Am J Anat* **12**, 1–26.

Pooh RK, Shiota K, Kurjak A (2011) Imaging of the human embryo with magnetic resonance imaging microscopy and high-resolution transvaginal 3-dimensional sonography: human embryology in the 21st century. *Am J Obstet Gynecol* **204**, 77.e1–77.e16.

van der Putte SC (1986) Normal and abnormal development of the anorectum. *J Pediatr Surg* **21**, 434–440.

van der Putte SC (2004) *The Development of the Perineum in the Human : A Comprehensive Histological Study with a Special Reference to the Role of the Stromal Components*. New York: Springer.

van der Putte SC (2006) Anal and ano-urogenital malformations: a histopathological study of "Imperforate Anus" with a reconstruction of the pathogenesis. *Pediatr Dev Pathol* **9**, 280–296.

van der Putte SC (2009) The development of the human anorectum. *Anat Rec (Hoboken)* **292**, 951–954.

van der Putte SC, Neeteson FA (1983) The normal development of the anorectum in the pig. *Acta Morphol Neerl Scand* **21**, 107–132.

van der Putte SC, Neeteson FA (1984) The pathogenesis of hereditary congenital malformations of the anorectum in the pig. *Acta Morphol Neerl Scand* **22**, 17–40.

Quan BQ, Beasley SW, Williams AK, et al. (2000) Does the urorectal septum fuse with the cloacal membrane? *J Urol* **164**, 2070–2072.

Rathke H (1832) *Abhandlungen zur Bildungs- und Entwicklungsgeschichte des Menschen und der Thiere 1. Theil*. Leipzig: Theil.

Reichel P (1893) Die Entwicklung der Harnblase und Harnröhre. *Phys-Med Gesell zu Würzburg* **27**, 1–41.

Reichmann S, Lewin T (1971) The development of the lumbar lordosis. *Arch Orthop Unfall-Chir* **69**, 275–285.

Retterer E (1890) Sur l'origine et l'evolution de la region anogenitale des mammiferes. *J Anat Physiol* **26**, 126–216.

Runck LA, Method A, Bischoff A, et al. (2014) Defining the molecular pathologies in cloaca malformation: similarities between mouse and human. *Dis Model Mech* **7**, 483–493.

Saguintaah M, Couture A, Veyrac C, et al. (2002) MRI of the fetal gastrointestinal tract. *Pediatr Radiol* **32**, 395–404.

Sasaki C, Yamaguchi K, Akita K (2004) Spatiotemporal distribution of apoptosis during normal cloacal development in mice. *Anat Rec A Discov Mol Cell Evol Biol* **279A**, 761–767.

Schoenwolf GC, Bleyl SB, Brauer PR, et al. (2015) *Larsen's Human Embryology*. Philadelphia, PA: Elsevier/Churchill Livingstone.

Seifert AW, Harfe BD, Cohn MJ (2008) Cell lineage analysis demonstrates an endodermal origin of the distal urethra and perineum. *Dev Biol* **318**, 143–152.

Seifert AW, Bouldin CM, Choi K-S, et al. (2009) Multiphasic and tissue-specific roles of sonic hedgehog in cloacal septation and external genitalia development. *Development* **136**, 3949–3957.

Smith ED, Stephens FD (1988) High, intermediate, and low anomalies in the male. *Birth Defects Orig Artic Ser* **24**, 17–72.

Soffers JH, Hikspoors JP, Mekonen HK, et al. (2015) The growth pattern of the human intestine and its mesentery. *BMC Dev Biol* **15**, 31.

Stephens FD (1988) Embryology of the cloaca and embryogenesis of anorectal malformations. *Birth Defects Orig Artic Ser* **24**, 177–209.

Tanaka ST, Ishii K, Demarco RT, et al. (2010) Endodermal origin of bladder trigone inferred from mesenchymal-epithelial interaction. *J Urol* **183**, 386–391.

Tobin CE, Benjamin JA (1945) Anatomical and surgical restudy of Denonvilliers' fascia. *Surg Gynec Obst* **80**, 373–388.

Tourneux F (1888) Sur les premiers developpements du cloaque du turbercule genital et de l'anus chez l'embryon de mouton. *J Anat Physiol* **24**, 503–517.

Treuting PM, Dintzis SM (2012) Lower gastrointestinal tract. In: *Anatomy and Histology – A Mouse and Human Atlas*. (eds Treuting PM, Dintzis SM), pp. 177–192. Amsterdam: Academic Press.

Tschopp P, Sherratt E, Sanger TJ, et al. (2014) A relative shift in cloacal location repositions external genitalia in amniote evolution. *Nature* **516**, 391.

Uhlenhuth E, Wolfe W, Smith E, et al. (1948) The rectogenital septum. *Surg Gynec Obst* **86**, 148–163.

van de Ven C, Bialecka M, Neijts R, et al. (2011) Concerted involvement of Cdx/Hox genes and Wnt signaling in morphogenesis of the caudal neural tube and cloacal derivatives from the posterior growth zone. *Development* **138**, 3859.

Viana R, Batourina E, Huang H, et al. (2007) The development of the bladder trigone, the center of the anti-reflux mechanism. *Development* **134**, 3763–3769.

de Vries PA (1988) High, intermediate, and low anomalies in the female. *Birth Defects Orig Artic Ser* **24**, 73–98.

van der Werff JF, Nievelstein RA, Brands E, et al. (2000) Normal development of the male anterior urethra. *Teratology* **61**, 172–183.

Wilkinson AW (1972) Congenital anomalies of the anus and rectum. *Arch Dis Child* **47**, 960–969.

Xu K, Wu X, Shapiro E, et al. (2012) Bmp7 functions via a polarity mechanism to promote cloacal septation. *PLoS One* **7**, e29372.

Yamaguchi K, Kiyokawa J, Akita K (2008) Developmental processes and ectodermal contribution to the anal canal in mice. *Ann Anat* **190**, 119–128.

Zhang T, Zhang HL, Wang DJ, et al. (2011) Normal development of hindgut and anorectum in human embryo. *Int J Colorectal Dis* **26**, 109–116.

Supporting Information

Additional Supporting Information may be found in the online version of this article:

Fig. S1. Brief procedure of 3D analysis.

Fig. S2. Semilogarithmic plots of growth in the cloacal region.

Fig. S3. Zonation of anorectal canal.

Fig. S4. 3D pdfs of the cloacal region from CS11 to CS14.

Fig. S5. 3D pdfs of the lateral folds from CS13 to CS14.

Fig. S6. 3D pdfs of the cloacal region from CS15 to CS23.